Atmósfera (2000) 13, pp. 185-195

The modulation of deep convection over the Gulf of Tehuantepec by easterly waves

JOSEPH A. ZEHNDER, GILBERTO VELAZQUEZ, AND LUIS M. FARFAN

University of Arizona, Department of Atmospheric Sciences, Tucson, AZ 85721-0081, USA

(Manuscript received Aug. 6, 1999; accepted in final form Sept. 25, 1999)

RESUMEN

Este artículo examina la relación entre ondas del este que se propagan desde el mar Caribe hacia el este del océano Pacífico y estallidos de convección intensa que con frecuencia ocurren sobre el Golfo de Tehuantepec y se intensifican en ciclones tropicales. El estudio muestra que hay perturbaciones sobre el Caribe a la vez que la convección se desarrolla sobre el Golfo y que estas perturbaciones tienen estructura horizontal y vertical y facciones de la propagación que son características de ondas del este.

ABSTRACT

This paper examines the relation between easterly waves that propagate from over the Caribbean Sea toward the East Pacific Ocean and deep convective bursts that frequently occur over the Gulf of Tehuantepec and often intensify into tropical cyclones. This study shows that there are disturbances present over the Caribbean at the time the convection is developing over the Gulf and that the disturbances have a horizontal and vertical structure and propagation features characteristic of easterly waves.

1. Introduction

The tropical East Pacific, just west of the coasts of Mexico and Central America, experiences one of the highest frequencies of tropical cyclogenesis in the world (Renard and Bowman, 1976). The reason for the existence of this preferred geographic location is the subject of debate, but most theories involve the presence of easterly waves that propagate into the region from the Caribbean (e.g., Rappaport and Mayfield, 1992). The mechanism by which the cyclonic relative vorticity associated with the wave is reduced in horizontal scale and increased in magnitude is still under investigation.

The origin, structure, and propagation characteristics of easterly waves are well documented in the literature. These waves originate over Africa and are the result of barotropic instability of the African easterly jet (Burpee, 1972). The structure of the waves is described by Reed *et al.* (1977), who used GATE data to construct composites of the wind and relative vorticity distributions. Easterly waves have a wavelength of about 2500 km and a maximum amplitude at about the 600-mb level, being cold core below and warm core above. There is also an orientation of the mid-level trough axis from southwest to northeast. The waves also have periods on the order of 3-5 days (Shapiro, 1986). This period corresponds to a propagation speed of about $6^{\circ}$of longitude day^{-1}.

In a recent study, Zehnder *et al.* (1999) suggest that the genesis of tropical cyclones in the East Pacific results from a mutual interaction between the easterly waves, the orography of Mexico and Central America, and the monsoon trough or ITCZ. Zehnder *et al.* (1999), describe a mechanism through which the waves are intensified by interacting with the orography, and the enhanced wave subsequently perturbs the monsoon trough. They also present a case study based on satellite imagery, which shows that a precursor of a tropical cyclone is a region of deep convection that develops over the Gulf of Tehuantepec (14-16°N, 92-96°W). A key feature of the mechanism described by Zehnder *et al.* (1999), is that the primary wave trough is upstream at the time that the deep convection on the lee side and accompanying vorticity maximum begin to develop.

The mechanism described by Zehnder *et al.* (1999) is a generalization of one described by Farfan and Zehnder (1997) (hereafter referred to as FZ97) as part of a case study of the genesis of hurricane Guillermo (1991). FZ97 show that as an easterly wave approaches from the east, there is a change in the incident low-level wind such that the flow impinges on the terrain. This results in a splitting of the flow around the south edge of the Central American mountains and the formation of a southeasterly jet along the coast and to the south of the Gulf of Tehuantepec. There is also a funneling of the flow through the Isthmus of Tehuantepec, which results in the formation of a north-easterly jet to the west of the coastal jet. These two flow features, along with the southwesterlies associated with the East Pacific monsoon trough, formed the first evidence of a closed circulation that eventually intensified into hurricane Guillermo. In FZ97 the key feature is once again the location of the primary trough axis upstream at the time the circulation is developing over the Gulf of Tehuantepec.

Another example of an easterly wave-induced case of East Pacific cyclogenesis is discussed by Molinari *et al.* (1999). They showed that an easterly wave which could be traced back to Africa resulted in an enhanced flow through the Isthmus of Tehuantepec. This flow resulted in an increase in the relative vorticity over the Gulf of Tehuantepec and the subsequent formation of Hurricane Hernan (1996).

The relation between upstream disturbances and the formation of circulations in the East Pacific was also demonstrated by Raymond *et al.* (1998). They examined time-longitude sections of IR brightness temperatures over a latitude band from 9°N-14°N and showed that each of the

East Pacific disturbances that occurred during July and August of 1991 could be traced to a convective maximum east of 90°W longitude.

The purpose of this note is to further examine the relation between the easterly waves approaching the East Pacific from the Caribbean and the subsequent formation of deep convection over the Gulf of Tehuantepec. We will consider the same time period as in Raymond *et al.* (1998) and emphasize the location of the upstream disturbances at the time that the convection is developing over the Gulf. The analysis is performed using an objective method for identifying loosely organized cloud clusters over the Caribbean that are associated with the easterly waves and correlating these with the occurrence of deep convection downstream. We will also demonstrate that there are synoptic-scale circulation features associated with the upstream cloud clusters that are suggestive of the easterly waves described by Reed *et al.* (1977).

2. Data

The period of interest is 1 July through 15 August, 1991. This period was chosen since it coincides with the TEXMEX experiment (Renno *et al.*, 1992) and the necessary data were readily available. One source of data is IR images from GOES-7. At that time, there was a single GOES satellite operational, and it was located directly over the East Pacific. The GOES-IR images have an 8-km resolution, with areal coverage from 7°N to 55°N and from 60°W to 140°W. Time series of the areal averaged IR brightness temperatures are constructed using hourly images. A 24-hour running mean was calculated in order to remove short time-scale variations and any signal due to the diurnal convective cycle.

Brightness temperatures are obtained from calibration relations that are based on tables supplied by the NOAA Sensor Calibration Section. These tables provide an operational relation between image gray level (GL) and black-body temperature (T) (Clark, 1983). The relation between the gray level and brightness temperature is approximated using the following relations

$$T = (-0.5)GL + 330 \qquad 0 \leq GL \leq 175 \tag{1a}$$

$$T = (-1.0)GL + 418 \qquad 176 \leq GL \leq 255 \tag{1b}$$

where T is in units of K.

A second source of data is the global analyses from the European Centre for Medium-Range Weather Forecasts (ECMWF). The data have a spectral triangular truncation at wavenumber 106. This truncation is equivalent to a horizontal resolution of about 1.125 degrees of latitude in the region of interest in this study. The fields were available at 6-hourly intervals, starting at 00 UTC. Reed *et al.* (1988) showed that the ECMWF analysis is useful in tracking easterly waves, particularly at the 850-mb level.

3. Correlation between easterly waves and deep convection over the East Pacific

The easterly waves in the Caribbean and accompanying deep convection over the Gulf of Tehuantepec will be identified through areal averages of the IR brightness temperature obtained from the GOES-IR imagery as described in section 2. The regions over which the averaging is performed are shown in Figure 1. The motivation for the choice of these regions is that minima in the IR brightness temperature correspond to maxima in convection that are associated with either easterly waves or the deep convective bursts over the Gulf of Tehuantepec.

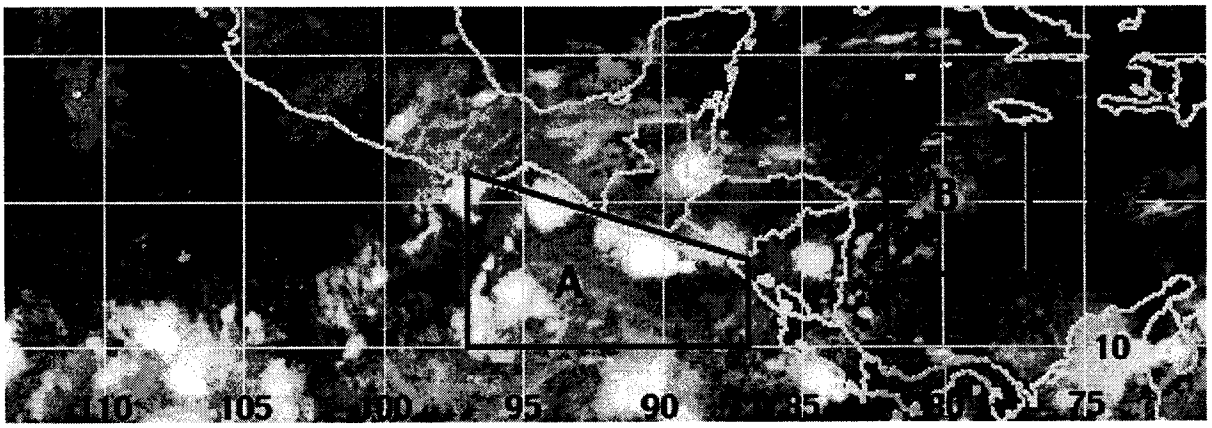

Fig. 1. Geographical location of the east Pacific (A) and Caribbean (B) regions used for calculation of the areal-averaged brightness temperatures. This scene shows an example of the relative distributions of deep convection (A) and loosely organized convection associated with easterly waves (B).

The downstream region (A in Fig. 1) was chosen due to the frequent occurrence of deep convection (e.g., Zehnder *et al.*, 1999, Fig. 1). The upstream region (B in Fig. 1) was located at a characteristic central latitude for easterly waves. The region was also centered to the east of the continental land mass. This location was chosen to avoid confusion between minima in the IR brightness temperature associated with easterly waves and those associated with the diurnal convective maximum over Mexico and Central America (Negri *et al.*, 1994).

Plots of the areal-averaged IR brightness temperature in the regions described above are shown in Figure 2a. There are 5 distinct minima in IR brightness temperature in region A that correspond to deep convective bursts over the Gulf of Tehuantepec. The last three of the minima were followed, within a day or two, by identification of a circulation that eventually intensified into a hurricane. The initial locations of Fefa (10.8°N, 107.2°W) Guillermo (12.3°N, 98.4°W), and Hilda (13.3°N, 101.9°W) are consistent with cloud clusters that originate in region A. The other named storm that formed during the period under consideration, Enrique (9.4°N, 111.9°W), was located rather far west and hence is not consistent with the scenario described by Zehnder *et al.* (1999).

The time series in region B has a series of minima in brightness temperature similar to that in region A; but the temperatures are generally higher, and there is less variability between the maximum and minimum values. The generally high brightness temperatures are the result of the convection being less well organized in the easterly waves while they are upstream of the continent. There is a fair amount of relatively clear air between the convective cells. In contrast, the downstream region tends to be filled with deep convection and relatively little clear air. An example of the relative amount of cloud coverage in regions A and B is shown in Figure 1.

In order to demonstrate the relation between upstream and downstream convection, it would be necessary to match the minima in the up- and downstream regions. A matching of that sort would be somewhat subjective. Instead, we will consider a time-lagged correlation between the two time series. A linear correlation coefficient is evaluated with a successive forward shift of the series in region B, using the standard expression given by Press *et al.* (1992). For a given time lag, τ the correlation coefficient, r is given by

$$r(\tau) = \frac{\sum_{i=1+\tau}^{N-\tau}(x_{i-\tau} - \overline{x})(y_i - \overline{y})}{\sqrt{\sum_{i=1+\tau}^{N-\tau}(x_{i-\tau} - \overline{x})^2}\sqrt{\sum_{i=1+\tau}^{N-\tau}(y_i - \overline{y})^2}} \tag{2}$$

where x and y represent the time series in regions A and B respectively and the overbar represent a mean over the interval $i = 1 + \tau,\ N - \tau$.

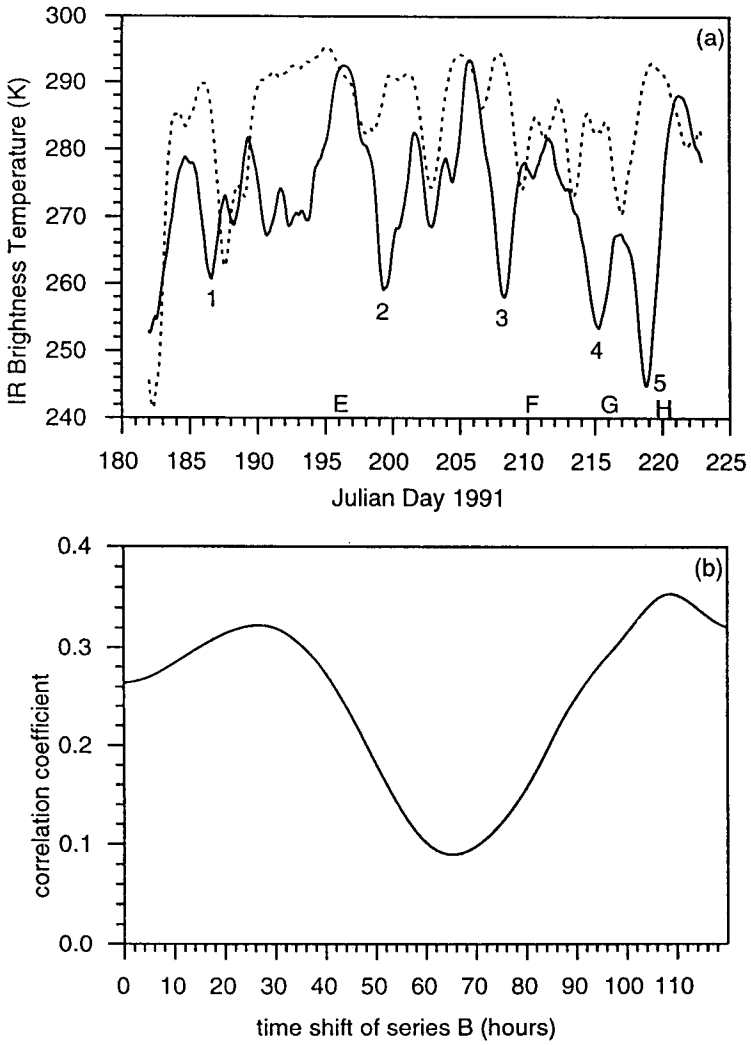

Fig. 2. (a) Time series of areal-averaged IR brightness temperature (K) for region A (solid) and region B (dashed) defined in Figure 1. The letters indicate the dates of formation of hurricanes Enrique, Fefa, Guillermo, and Hilda. (b) Linear correlation coefficient of times series as a function of forward displacement of series in Region B.

The correlation coefficient as a function of time shift is shown in Figure 2b. There are maxima in the correlation coefficient for forward time shifts of $t = 27$ hours and $t = 110$ hours. The timing of the first maxima of the correlation coefficient shown in Figure 2b is consistent with the mechanism described in Zehnder *et al.* (1999). The interpretation of the time shift is that the minima in brightness temperature over the Caribbean leads the deep convection over the Gulf of Tehuantepec by 27 hours. If we assume that the wave is centered in region B at the time corresponding to the maximum in the correlation coefficient and that the wave propagates at 6° latitude day^{-1}, then the wave trough would be located just east of the coast of Central America at the time the deep convection over the Gulf of Tehuantepec occurs. This position of the wave trough is consistent with that shown by Zehnder *et al.* (1999) in their Figure 2.

The second maximum in the correlation occurs at t =110 hours, which is approximately 5 days. This time frame is consistent with the period of the easterly waves, so it is interpreted as aliasing with the next wave in the sequence. It is noted that the correlation coefficient is slightly higher for the second maximum (.35 as compared with .32 for the primary maximum). This is likely due to the relatively short time period under consideration.

4. Upstream circulations associated with deep convection over the East Pacific

In the preceding section, we demonstrated that there are convective maxima located over the Caribbean that are associated with deep convection over the Gulf of Tehuantepec. In this section, we will examine the structure of the circulation features that are associated with upstream cloud clusters by constructing composite wind and vorticity fields. The fields from which the composites are constructed were chosen based on the time series analysis presented in section 3.

The composite wind and vorticity maxima are weak, due to variations in the latitudinal and longitudinal position of the waves at the time the gridded fields are available. Reed *et al.* (1977) overcame this problem by combining the waves in a coordinate system that was defined relative to the wave axis. The Reed *et al.* (1977) method cannot be applied here, since we are interested in the location of the waves relative to the terrain. The weak wave signature is further obscured by the wind and relative vorticity associated with the basic state. Since we are interested in the position of the waves relative to the terrain, we will construct simple composites and highlight the wind and vorticity distributions associated with the waves by presenting anomaly fields. The anomaly fields will be determined by combining the wave events and subtracting the mean field determined for the period of interest.

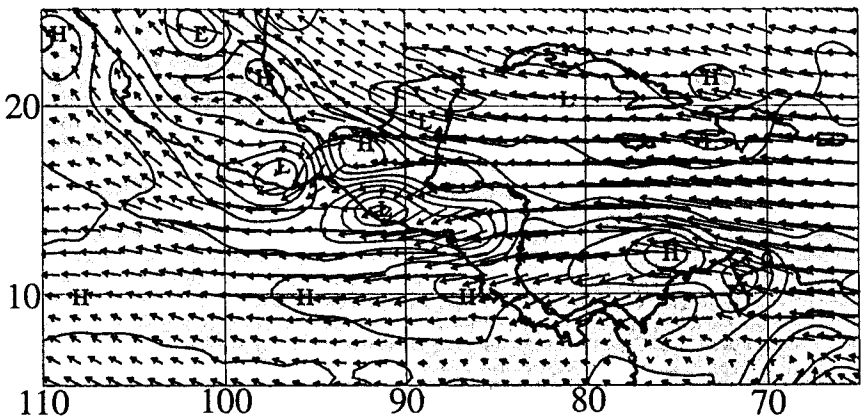

Fig. 3. Average wind and relative vorticity at 850-m b level for the period 1 July 15 August 1991. Maximum wind vector is 15 ms^{-1}, and relative vorticity contours are 1×10^{-5} s^{-1}. Shaded regions indicate cyclonic relative vorticity.

The mean 850-mb wind and relative vorticity distributions are shown in Figure 3. The basic state is derived by combining the fields at six-hour intervals for the period 1 July - 15 August, 1991. The wind and relative vorticity fields shown in Figure 3 are consistent with climatological fields calculated for longer time periods (Hastenrath and Lamb, 1978). The mean winds at this level are predominantly easterly, with a shift to southeasterlies along the east coast of Mexico. The southeasterlies are associated with the western edge of the Bermuda High, and it is the shift of the wind in this region to northeasterly that is responsible for the flow splitting and cyclogenesis over the Gulf of Tehuantepec as described in FZ97. The mean state relative

vorticity is cyclonic in a band along roughly 10°N. This vorticity maximum marks the mean location of the ITCZ in the region. It is also noted that the mean state relative vorticity east of the Yucatan Peninsula and south of Cuba is anticyclonic. It is in this region that the cyclonic relative vorticity anomalies associated with the waves should be present.

Anomaly fields were constructed by combining the 850-mb wind and relative vorticity at times 24 hours prior to the five minima of IR brightness temperature in Region A shown in Figure 2a. This time shift was chosen since it corresponds to the first maxima in the time lagged correlation coefficient between brightness temperatures upstream and downstream shown in Figure 2b. The anomaly fields are presented in Figure 4a. This figure shows clear evidence of a cyclonic vorticity anomaly with a structure suggestive of an easterly wave located upstream of Central America at the time that the deep convection is beginning over region A. This anomaly is centered at 15°N, 82°W and has a horizontal scale of about 1000 km.

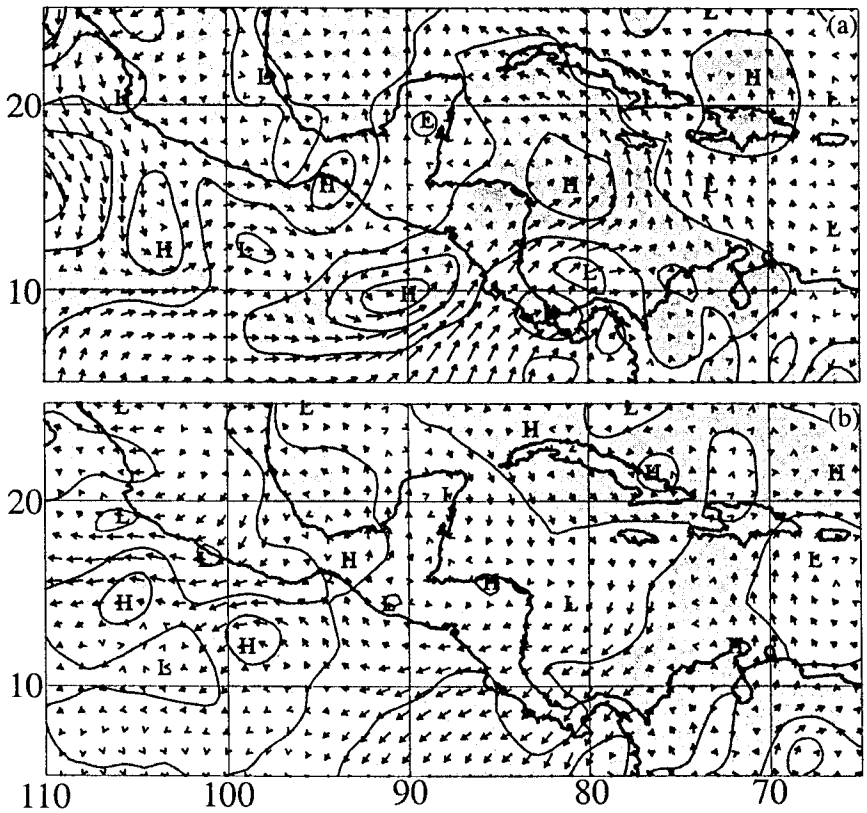

Fig. 4. Wind and relative vorticity anomalies at 850 mb 24 hours prior to the (a) four minima and (b) six maxima in IR brightness over Region A. Maximum wind vector is 5 m s^{-1}, and relative vorticity contours are 1×10^{-5} s^{-1} 1. Shaded regions indicate cyclonic relative vorticity.

In addition to the cyclonic anomaly present over the Caribbean, there are also a number of small-scale vorticity maxima located over the East Pacific. These features are due to the presence of hurricanes at the time that other waves in the sequence are approaching the region. For example, the cyclonic vorticity anomaly located at 12°N and 105°W is associated with Hurricane Guillermo. Guillermo is present at the time that the wave associated with Hurricane Hilda approaches the continent, and hence it appears in the composite field. Also, the elongated vorticity maxima that are centered at around 90° W seem to be associated with the intensification of the ITCZ southerlies in the presence of the wave that is described in FZ97.

As a basis of comparison with the wave composite shown in Fig. 4a, we construct a composite of the anomaly fields for the days corresponding to the six maxima in IR brightness temperature over region A shown in Figure 2a. This composite is shown in Figure 4b. In this case, there is a negative relative vorticity anomaly to the east of the Yucatan Peninsula and no evidence of an easterly wave as in Figure 4a. There are some small-scale vorticity anomalies located west of 100°W, but there is no evidence of the anomalously strong ITCZ, as in Figure 4a.

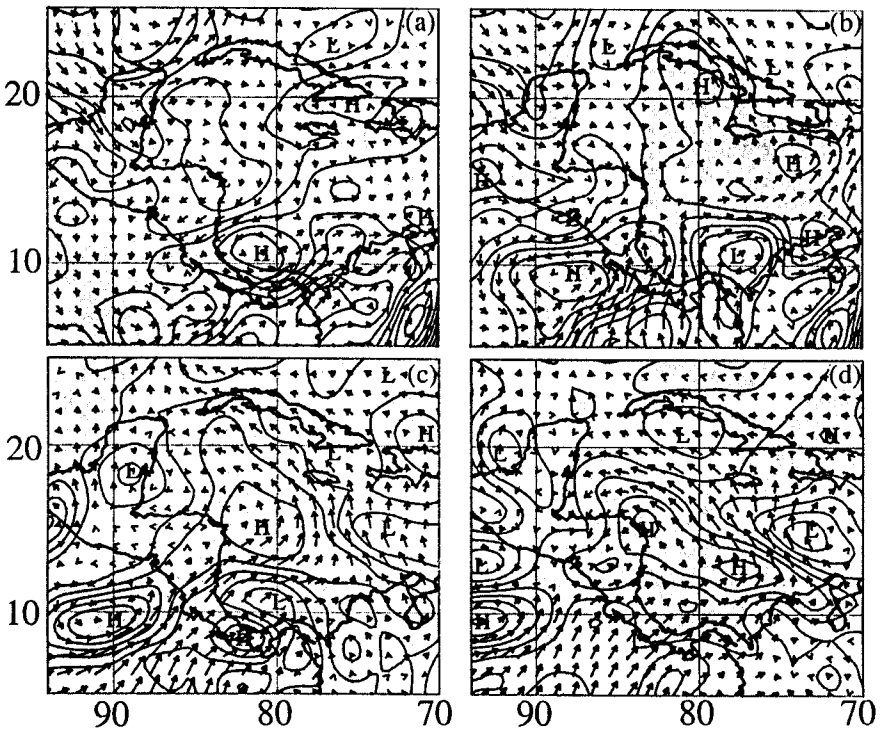

Fig. 5. Wind and relative vorticity anomalies at 850 mb (a) 48 hours, (b) 36 hours, (c) 24 hours, and (d) 12 hours prior to the four minima in IR brightness over Region A. Wind vectors and relative vorticity contours are as in Fig. 4.

The horizontal scale of the cyclonic vorticity shown in Figure 4a is suggestive of the Reed *et al.* (1977) composite easterly wave. However, if this feature is associated with an easterly wave, there should be some evidence of propagation. We will estimate the propagation of the feature by constructing composite fields at 12-hour intervals prior to and following times used to construct the anomaly fields in Figure 4a. The series of composite fields is shown in Figure 5.

At 48 hours prior to the deep convective bursts over the Gulf of Tehuantepec, there is a fairly complicated distribution of relative vorticity at the 850-mb level (Fig. 5a). The region just to the east of the Yucatan peninsula has anticyclonic relative vorticity, and there is cyclonic relative vorticity to the east, centered at about 75°W. There are also two vorticity anomalies, one located at 15°N and the other at about 20°N. This is likely due to variability in the latitudinal position of the waves that make up the composite. The movement of this pattern toward the west can be seen at 36 hours prior to the convective maxima (Fig. 5b). Figure 5c shows the relative vorticity maxima at 24 hours prior to the convective maxima as a basis for comparison. At 12 hours prior to the brightness temperature minima, the cyclonic anomaly is further west than at the preceding time.

The sequence of relative vorticity anomalies shown in Figure 5 suggests the propagation of a synoptic-scale relative vorticity anomaly toward the west. The anomaly moves about 10° toward the west in 36 hours, which corresponds to roughly $6°\text{day}^{-1}$. This speed agrees with the characteristic easterly wave propagation speed. Granted, there are a number of other vorticity anomalies present to the south and west of the waves being discussed above. These are due to the aliasing problem referred to above. However, it is noted that there is a cyclonic vorticity anomaly in the Caribbean at the time the deep convection is developing downstream. This would not occur if the deep convection were entirely independent of the upstream circulation, i.e., if the development were due simply to vorticity being advected at low latitudes or forming *in situ*.

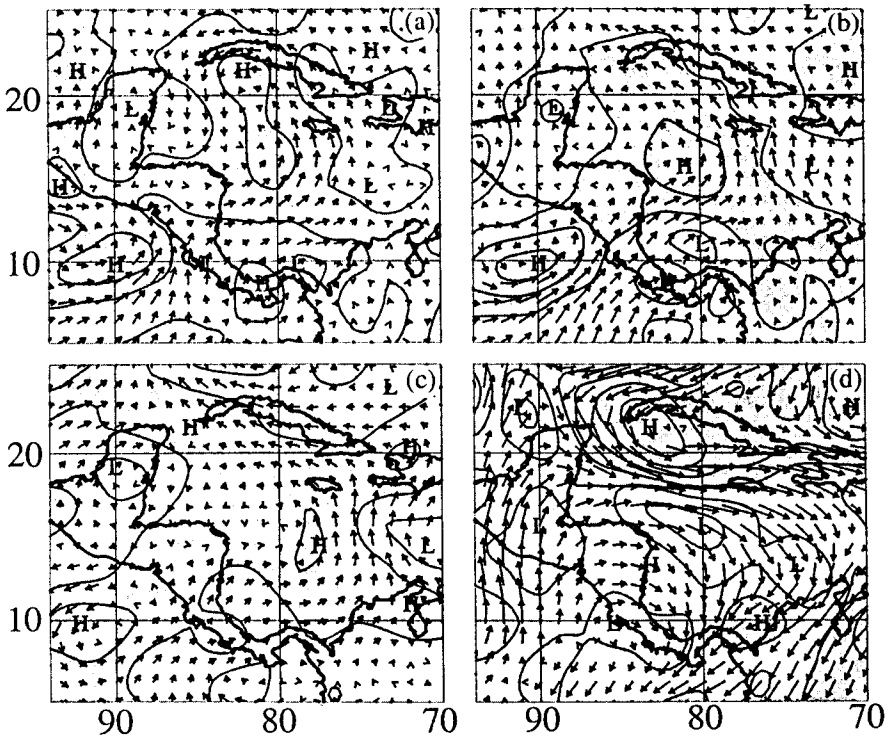

Fig. 6. Wind and relative vorticity anomalies 24 hours prior to the four minima in IR brightness over Region A at (a) 1000 mb, (b) 850 mb, (c) 700 mb, and (d) 200 mb. Wind vectors and relative vorticity contours are as in Fig. 4.

Further evidence that the composite structure is associated with easterly waves is obtained by considering the vertical structure. Figure 6 shows the relative vorticity at a series of levels from 1000 to 200 mb. The composite wave in the Caribbean seems to be decreasing in amplitude above the 850-mb level, and the anomaly eventually becomes anticyclonic at the 200-mb level. Again, the relative vorticity distribution is complicated due to the relatively small sample size, but the composites suggest a structure that is cold core below the middle troposphere and warm core above, which is consistent with the composite easterly wave structure described by Reed *et al.* (1977).

5. Conclusions

The analysis presented in the preceding sections shows that there is a relation between deep convective bursts over the Gulf of Tehuantepec, as reflected through minima in the IR brightness temperature averaged over the region. These convective bursts are preceded by loosely organized convection over the Caribbean. The time series of IR brightness temperature suggests that there is a disturbance upstream at the time that the deep convection is developing downstream. Composites of the wind and relative vorticity suggest a synoptic-scale structure that propagates toward the west at a speed of 6°day^{-1} and is cold core below and warm core above the mid-troposphere. The motion and structure of the disturbance is suggestive of easterly waves, which have long been associated with East Pacific cyclogenesis (e.g., Rappaport and Mayfield, 1992). The analysis also indicates that the wave is located upstream of the Yucatan Peninsula at the time the downstream convection is developing, which is consistent with the mechanism described by Farfan and Zehnder (1997) and Zehnder *et al.* (1999).

The results presented here are by no means conclusive, but suggest an area which should be explored further. There are many more easterly waves analyzed in any given year than East Pacific tropical cyclones. An accounting of the numbers of tropical cyclones that can be traced back to the convective bursts over the Gulf of Tehuantepec is necessary. In this way, we may partition the cases between developing and nondeveloping and identify development criteria. Some possibilities are the structure, strength, and variation of the central latitude of the easterly waves. It is also possible that the characteristics of the environment (such as the distribution of relative vorticity or location of the East Pacific ITCZ) may determine which of the cloud clusters subsequently intensify. The combination of easterly wave analysis and criteria for the intensification will provide the opportunity for forecasting the genesis of East Pacific tropical cyclones. This may provide additional lead times for landfall warning on the east coast of Mexico.

Acknowledgments

Partial support for this work was provided under NOAA Grant NA56GP0189 and NSF Grant ATM-9412751.

REFERENCES

Burpee, R. W., 1972. The origin and structure of easterly waves in the lower troposphere of North Africa. *J. Atmos. Sci.*, **29**, 77-90.

Clark, J. D., 1983. *The GOES Users' Guide.* NOAA/NESDIS, 169 pp.

Farfan, L. M., and J. A. Zehnder, 1997. Orographic influence on the synoptic-scale circulations associated with the genesis of hurricane Guillermo (1991). *Mon. Wea Rev.*, **125**, 2683-2698.

Hastenrath, S., and P. Lamb, 1978. On the dynamics and climatology of surface flow over the equatorial oceans. *Tellus*, **30**, 436-448.

Molinari, J., D. Vollaro, S. Skubis, and M. Dickenson, 2000. Origins and mechanisms of Eastern Pacific tropical cyclogenesis: A case study. *Mon. Wea. Rev.*, **128**, 125-139.

Negri, A. J., R. F. Adler, E. J. Nelkin, and G. J. Huffman, 1994. Regional rainfall climatologies from Special Sensor Microwave Imager (SSM/I) data. *Bull. Am. Met. Soc.*, **75**, 1165-1182.

Press, W. H., S. A. Teukolsky, W. T. Vetterling, and B. P. Flannery, 1992. *Numerical Recipes in Fortran: The Art of Scientific Computing.* Cambridge University Press, Second Ed., 963 pp.

Rappaport, E. N., and M. Mayfield, 1992. Eastern North Pacific hurricane season of 1991. *Mon. Wea. Rev.*, **120**, 2697-2708.

Raymond, D. J., C. López-Carrillo, and L. López-Cavazos, 1998. Case-studies of developing east Pacific easterly waves. *Quart. J. Roy. Met. Soc.*, **124**, 2005-2034.

Reed, R. J., D. C. Norquist, and E. E. Recker, 1977. The structure and properties of African wave disturbances as observed during phase III of GATE. *Mon. Wea. Rev.*, **105**, 317-333.

Reed, R. J., A. Hollingsworth, W. A. Heckley, and F. Delsol, 1988. An evaluation of the performance of the ECMWF operational system in analyzing and forecasting easterly wave disturbances over Africa and the tropical Atlantic. *Mon. Wea. Rev.*, **116**, 824-865.

Renard, R. J., and W. N. Bowman, 1976. The climatology and forecasting of eastern North Pacific ocean tropical cyclones. NEPRF Tech. Paper No. 7-76, 79 pp.

Rennó, N., L. Schade, M. Morgan, M. Bister, C. Wu, and D. Reilly, 1992. TEXMEX data report. Massachusetts Institute of Technology, 180 pp. [Available from CMPO/MIT, Cambridge, MA 02139.]

Shapiro, L. J., 1986. The three dimensional structure of synoptic scale disturbances over the tropical Atlantic. *Mon. Wea. Rev.*, **114**, 1876-1891.

Zehnder, J. A., D. Powell, and D. Ropp, 1999. The interaction of easterly waves, orography and the Inter-tropical Convergence Zone in the genesis of eastern Pacific tropical cyclones. *Mon. Wea. Rev.*, **127**, 1566-1585.